Journal of Theoretical and Applied Information Technology
31st March 2026. Vol.104. No.6

ISSN: 1992-8645 www.jatit.org E-ISSN: 1817-3195

KRILL HERD OPTIMIZED ZONE ROUTING PROTOCOL (KHO-ZRP) FOR ENERGY-EFFICIENT ULTRA-DYNAMIC FLYING AD HOC NETWORKS

GUNAVATHY H[1] , Dr.RAVINDRANATH P.V[2]
[1]Research Scholar, School of Computer Science (PG), RVS College of Arts & Science, Sulur, Coimbatore, Tamil Nadu, India
[2]Assistant Professor, School of Computer Science (PG), RVS College of Arts & Science, Sulur, Coimbatore, Tamil Nadu, India
E-mail: [1]gunahg.2014@gmail.com, [2]ravindranath@rvsgroup.com

ABSTRACT

Flying Ad Hoc Networks operate under extreme mobility, fluctuating node density, frequent link disruptions, and strict energy constraints, which jointly degrade routing stability and communication reliability. Existing FANET routing approaches address these challenges in isolation through learning-based adaptation, clustering, or bio-inspired heuristics, leaving coordination among zoning, relay selection, and energy regulation insufficiently explored. This work introduces a Krill Herd Optimized Zone Routing Protocol that embeds collective swarm intelligence directly into zonal routing control. New knowledge is created through an optimization-governed routing framework where krill herd dynamics regulate zone radius adaptation, relay selection, hop progression, and spatial stability within a unified routing architecture. The contribution advances routing-system design rather than proposing a new optimizer, enabling stable and energy-aware communication under ultra-dynamic aerial conditions. NS3-based evaluation across varying node densities demonstrates reduced delay, lower packet loss, improved packet delivery, higher throughput, and controlled energy consumption compared to existing protocols. Results confirm the effectiveness of optimization-driven zonal coordination for sustaining quality of service in highly dynamic FANET deployments.
Keywords: *Zone Routing Protocol, Krill Herd Optimization, UAV, FANET, QoS)*

1. INTRODUCTION

Flying Ad Hoc Networks (FANETs) present a challenging environment for communication systems, characterized by the dynamic movement of unmanned aerial vehicles (UAVs) operating in varying node densities [1]. The design and implementation of efficient routing protocols tailored to the unique characteristics of FANETs are essential to ensure reliable and timely communication among UAVs in these dynamic aerial environments. Traditional routing protocols developed for terrestrial networks are ill-suited for FANETs due to the distinct challenges posed by aerial operations. In FANETs, UAVs are subject to rapid mobility, variable node densities, limited energy resources, and potential interference from other UAVs or external sources [2]. These factors necessitate the development of innovative routing protocols capable of dynamically adapting to changing network conditions while optimizing communication paths and minimizing packet loss and delays [3].

Density-aware routing in FANETs is particularly crucial, as it enables UAVs to make informed routing decisions based on the density of nodes in their vicinity. By considering node density, routing protocols can optimize communication paths, minimize transmission overhead, and mitigate the risk of congestion in densely populated areas. Moreover, density-aware routing allows UAVs to dynamically adjust their routing strategies in response to changes in node density, ensuring efficient communication even as the network topology evolves [4]. To achieve density-aware routing in FANETs, researchers have explored various optimization techniques, machine-learning algorithms, and bio-inspired approaches. These include swarm intelligence, genetic algorithms, reinforcement learning, and Krill Herd Optimization (KHO). By integrating these techniques into routing protocols, researchers aim to develop adaptive and resilient solutions capable of autonomously adapting to dynamic network conditions, optimizing communication paths, and mitigating interference and collisions [5].

The advancements in communication technologies, such as the deployment of 5G and beyond, offer new opportunities for enhancing the capabilities of density-aware routing in FANETs [6]. These technologies provide high-speed data transmission, low-latency communication, and massive connectivity features, enabling UAVs to exchange large volumes of data in real-time and support various applications, including surveillance, disaster response, and environmental monitoring [7]. Density-aware routing is vital in optimizing communication performance and ensuring reliable connectivity in FANETs. By developing routing protocols that consider node density and dynamically adapt to changing network conditions, researchers can address the unique challenges of aerial environments and unlock the full potential of UAV-based communication networks for various applications. Continued research and innovation in this field are essential to advancing the state-of-the-art density-aware routing and realizing the vision of efficient and adaptive communication in FANETs [8], [9], [10].

This study contributes new knowledge by establishing an optimization-driven zonal routing framework explicitly tailored for ultra-dynamic Flying Ad Hoc Networks. The proposed KHO-ZRP framework formalizes the integration of krill herd swarm intelligence with zone-based routing to address simultaneous challenges of rapid mobility, fluctuating node density, frequent link disruptions, and strict energy constraints. Distinct from prior FANET routing studies that treat optimization and zonal routing as independent enhancements, the presented approach models krill movement dynamics as direct control mechanisms for zone radius adaptation, relay selection, hop regulation, and spatial stability enforcement. The scope of this contribution extends beyond performance improvement alone and introduces a structured methodology for embedding bio-inspired collective behavior into proactive–reactive hybrid routing architectures. Applicability spans surveillance swarms, emergency response UAV formations, border monitoring grids, and cooperative aerial missions operating under high mobility and density variability, where stable connectivity, energy sustainability, and routing predictability remain critical.

The central objective of this research is the design and evaluation of a krill herd–driven zonal routing framework capable of sustaining communication stability, energy efficiency, and quality of service under extreme FANET dynamics. The work targets controlled adaptation of zone radius, relay selection, hop progression, and route stability through bio-inspired collective behavior modeling. The research contribution is intentionally delimited to routing system design and optimization-guided parameter adaptation within the Zone Routing Protocol structure. The study does not aim to introduce a new swarm optimizer variant, mobility control mechanism, or physical-layer enhancement. Emphasis remains on routing-layer intelligence that translates krill herd dynamics into actionable routing decisions under rapid topology variation and density fluctuation. This delimitation ensures methodological clarity and positions the contribution as a system-level routing advancement for ultra-dynamic UAV networks.

1.1. Problem Statement

In FANET, efficient data transmission is pivotal for mission success. However, traditional routing protocols inadequately consider the dynamic nature of FANETs, where unmanned aerial vehicles (UAVs) operate in airspace characterized by varying node densities. The existing protocols often lack the sophistication to adapt to these dynamic conditions. The problem addressed in this research is the development of Density-Aware Routing (DAR) protocols, which aim to create routing strategies that intelligently adapt to changes in node density. These protocols need to dynamically select routes based on the density of nodes in the vicinity, optimizing data transmission efficiency in areas with variable network node distribution.

1.2. Motivation

The motivation for this research is rooted in the increasing application of FANETs across diverse missions, ranging from surveillance to disaster response. In these dynamic scenarios, UAVs must operate efficiently despite variations in node density. Traditional routing protocols often struggle to maintain data transmission reliability and efficiency in such conditions. The motivation is to develop DAR protocols that can adapt to the dynamic network topology, ensuring efficient

data transfer even in areas with sparse or dense node populations. By doing so, this research seeks to enhance the utility of FANETs across a range of applications, ensuring that they can consistently deliver data under changing network conditions, thereby increasing their reliability and effectiveness in dynamic, real-world missions.

1.3. Objective

The primary objective of this research is to design, implement, and evaluate Density-Aware Routing (DAR) protocols tailored to the dynamic challenges presented by FANETs. The study aims to address these specific technical objectives:

- Adaptive Routing Protocol Development: Develop advanced DAR protocols that integrate machine learning and artificial intelligence techniques to adapt to dynamic changes in node density within FANETs. These protocols should autonomously select routing paths based on real-time node density information, optimizing data transmission efficiency and minimizing routing overhead.
- Density Metrics and Prediction: To monitor and assess node sophisticated density measurement and prediction mechanisms, leveraging sensor data and predictive algorithms. This includes developing predictive models to anticipate changes in node density and plan routing strategies accordingly.
- Quality of Service (QoS) Optimization: Evaluate the performance of DAR protocols, focusing on QoS metrics such as latency, packet loss, and throughput. Optimize these protocols to provide enhanced QoS in areas with varying node density, ensuring that data transmission meets the stringent requirements of mission-critical applications.
- Dynamic Routing Strategy Selection: Investigate the adaptability and scalability of DAR protocols to respond to abrupt changes in node density. Develop routing strategy selection mechanisms that can efficiently switch between routing strategies, including proactive and reactive approaches, based on real-time assessments of node density.

These technically advanced research objectives aim to provide a more in-depth framework for developing Density-Aware Routing protocols, emphasizing adaptability, predictive capabilities, and QoS optimization in the challenging FANET environment characterized by dynamic node density variations.

1.4. Hypothesis

This work hypothesizes that routing instability, rising delay, packet loss, and energy drain in ultra-dynamic Flying Ad Hoc Networks originate from static zone configuration and non-adaptive relay selection under rapid mobility and density variation. It is assumed that routing performance can be significantly improved by coupling zone-based routing with bio-inspired collective optimization that continuously adapts zone radius, relay choice, and hop progression based on real-time spatial dynamics. The hypothesis frames routing inefficiency as a coordination problem rather than a connectivity problem, positioning adaptive optimization-driven zoning as a core mechanism for stabilizing communication and sustaining quality of service in highly dynamic UAV networks.

2. LITERATURE REVIEW

"SkyPaths" [11] protocol introduces a paradigm shift in Aeronautical Ad-Hoc Networks (AANETs) by integrating Q-learning for dynamic routing optimization. Q-learning, a reinforcement learning technique, is harnessed to enable UAVs to make intelligent decisions for communication paths in response to evolving network conditions. The protocol's core innovation lies in its adaptability, leveraging historical experiences to optimize communication paths in real-time dynamically. "K-Adapt UAV Route" [12] protocol addresses routing complexities in UAV ad-hoc networks by integrating K-means clustering and online learning. This innovative protocol dynamically adjusts routing decisions based on the shifting topologies of UAV networks, ensuring adaptability and efficiency. K-means clustering is employed to group UAVs with similar communication characteristics, forming clusters that streamline routing decisions within

each group. "SmartOptiUAV Clustering" [13] protocol introduces a novel and intelligent optimization approach tailored for clustering in UAV-assisted IoT wireless networks. In the context of IoT, where UAVs play a pivotal role, efficient clustering is essential for optimizing communication and resource utilization.

"UAV-Mobility Management" [14] protocol addresses the challenges of controlled mobility for UAVs within mobile heterogeneous wireless sensor networks. In the evolving landscape of wireless sensor networks, where UAVs are increasingly employed for data collection and communication, efficient mobility management is crucial. This protocol focuses on optimizing the controlled mobility of UAVs, ensuring strategic movement to enhance data collection efficiency and communication reliability. "Reinforce UAV Cluster Routing" [15] scheme represents a groundbreaking advancement in multi-UAV networks by incorporating a reinforcement learning-based approach for cluster routing with dynamic path planning. This protocol introduces a sophisticated solution in UAVs' dynamic and complex domain, where real-time decision-making and adaptability are paramount. By leveraging reinforcement learning, the scheme enables UAVs to learn and dynamically adjust their routing strategies based on evolving network conditions.

"Topology-Adapt FANET Routing" [16] protocol pioneers an adaptive Q-learning approach for resilient routing in FANETs. In the ever-changing and unpredictable environment of FANETs, this protocol introduces a resilient routing solution by integrating Q-learning with topology awareness. The adaptive Q-learning approach allows the protocol to optimize routing decisions based on the evolving network topology, ensuring adaptability to unforeseen changes. The protocol's nickname succinctly captures its essence. "Cluster Sky Routing" [17] protocol addresses the unique challenges of communication in Flying Ad Hoc Networks (FANETs) through a cluster-based routing approach. FANETs, characterized by dynamic and airborne communication scenarios, demand innovative solutions to optimize communication efficiency. This protocol strategically organizes Unmanned Aerial Vehicles (UAVs) into clusters, facilitating more efficient communication within each group. "AdaptFly Routing Design" [7] introduces a forward-thinking approach to routing in FANETs, emphasizing adaptability as a core design principle. Acknowledging the dynamic nature of airborne communication scenarios, this protocol integrates adaptability into its framework beyond conventional routing strategies. The adaptive routing design enables UAVs to dynamically adjust their routing decisions in response to real-time changes in the network environment.

"3DGeoRoute Protocol" [18] represents a significant leap forward in Three-Dimensional FANETs, introducing a pioneering geographical routing approach that considers the intricate spatial dimensions of airborne communication. In the dynamic and complex aerial environment, traditional two-dimensional routing protocols prove insufficient, necessitating novel strategies tailored for the three-dimensional space. "Reverse Glowworm Swarm Optimization" [19] introduces a sophisticated path-planning protocol for UAVs navigating dynamic three-dimensional spaces. Inspired by Reverse Glowworm Swarm Optimization (RGSO) principles, this protocol leverages swarm intelligence to guide UAVs through intricate and changing environments. "CovertComm in Multi-hop UAV Network" [20] protocol explores the intriguing domain of covert communication within multi-hop UAV networks, presenting innovative strategies to ensure discreet data transmission between UAVs. In scenarios where confidentiality and stealth are paramount, this protocol introduces covert communication techniques, allowing UAVs to maintain discreet interactions during multi-hop transmissions.

Bio-inspired optimization has emerged as a robust approach for solving complex networking problems by modeling adaptive behaviors observed in natural swarms [21]-[33]. In dynamic communication systems, swarm intelligence supports decentralized decision-making, continuous adaptation, and resilience under uncertainty. Such optimization paradigms are well suited for Flying Ad Hoc Networks, where rapid mobility, density variation, and frequent link changes demand responsive routing control [34]-[47]. By translating collective movement, local

interaction, and environmental awareness into algorithmic strategies, bio-inspired methods enable dynamic regulation of routing parameters, path stability, and energy usage [48]-[59]. This alignment makes swarm-based optimization an appropriate foundation for routing frameworks that seek to balance adaptability, efficiency, and stability in highly dynamic aerial network environments [60]-[63].

3. KRILL HERD OPTIMIZATION-INFUSED ZONE ROUTING PROTOCOL

Krill Herd Optimization-Infused Zone Routing Protocol (KHO-ZRP) is an innovative routing protocol designed for FANETs. Integrating Krill Herd Optimization (KHO) techniques into the Zone Routing Protocol (ZRP), KHO-ZRP enhances adaptability and efficiency in dynamic aerial environments. KHO draws inspiration from the collective behavior of krill swarms, employing optimization strategies to dynamically adjust routing decisions based on real-time factors such as node density and environmental conditions. By infusing KHO into ZRP, KHO-ZRP offers a robust solution for optimizing communication paths, minimizing delays, packet loss, and energy consumption in FANETs.

3.1. Initialization

The initial step in the KHO-ZRP algorithm is crucial for setting the foundation of the optimization process. In this step, we establish the network configuration, define parameters, and initialize variables required for subsequent computations. The mathematical representation of Initialization provides a clear framework for comprehending the foundational aspects of KHO-ZRP. Let N represent the total number of nodes in the network, Z denote the number of zones, and P symbolize the population size in the Krill Herd Optimization (KHO) algorithm. The initialization process begins by configuring the network, where each node i is assigned coordinates (x_i, y_i) within a predefined geographical area. This can be mathematically expressed as Eq.(1).

$$Node\ Coordinates: (x_i, y_i), \quad i = 1,2, \dots, N \tag{1}$$

The zones are defined to partition the network, with each node associated with a specific zone. The geographical proximity determines the assignment of nodes to zones, ensuring an efficient representation of local interactions within the KHO algorithm. The zone radius, denoted as R_z , influences the spatial coverage of each zone and is a critical parameter for the subsequent steps. Mathematically, the zone assignment can be expressed as Eq.(2).

$$Zone\ Assignment: Z_i = argmin_j \left(\sqrt{(x_i, x_j)^2 + (y_i, y_j)^2} \right), \quad i = 1,2,..,N \tag{2}$$

The KHO algorithm requires the Initialization of parameters specific to its optimization process. These include parameters governing krill individuals' movement and the solution space exploration. Let C_{max} denote the maximum speed of Krill, S_{max} represent the maximum step size, and β indicates the step size control parameter. The Initialization of these parameters can be expressed as Eq.(3).

$$Krill\ Speed: C_i = C_{max}.\left(1 - \frac{Z_i}{Z}\right), \quad i = 1,2, \dots, N$$
$$Step\ Size: S_i = S_{max}.\left(-\beta.\frac{Z_i}{Z}\right), \quad i = 1,2, \dots, N \tag{3}$$

The population size (P) in the KHO algorithm plays a pivotal role in determining the diversity of solutions explored during the optimization process. It represents the number of krill individuals in the population and is integral to the overall algorithmic performance. Mathematically, the Initialization of the population size is straightforward and expressed as Eq.(4).

$$Population\ Size: P = constant \tag{4}$$

By meticulously defining and initializing these network and algorithmic parameters, the Initialization step lays the groundwork for subsequent computations in the KHO-ZRP hybrid algorithm.

3.2. Define Objective Function

Building upon the Initialization step, the next crucial phase in the KHO-ZRP

algorithm involves precisely defining the objective function. The objective function serves as the mathematical representation of the optimization goals, incorporating both the inherent requirements of the Zone Routing Protocol (ZRP) and the overarching optimization objectives of Krill Herd Optimization (KHO). By formulating this objective function mathematically, we establish a clear framework for evaluating the fitness of potential solutions. Let f denote the objective function, which assesses the performance of the ZRP in the context of the specific optimization goals. The objective function captures various aspects such as energy efficiency, delay minimization, or packet delivery ratio. Its mathematical representation is expressed as Eq.(5).

$$f(ZRP) = w_1.F_1 + w_2.F_2 + \cdots . + w_m.F_m \quad (5)$$

where, F_i represents individual ZRP performance metrics, and w_i signifies the corresponding weights assigned to these metrics. The objective is to optimize a combination of factors that collectively contribute to the overall efficiency of the ZRP.

The KHO-ZRP algorithm introduces additional parameters that influence the objective function. Let W_{max} denote the maximum weight, W_{min} represent the minimum weight, and C_i signify the krill speed associated with node i. These parameters contribute to incorporating KHO's optimization characteristics into the ZRP framework. Mathematically, their roles in the objective function can be expressed as Eq.(6).

$$Weight\ Adjustment: w_i = W_{min} + \left(\frac{W_{max} - W_{min}}{N}\right).C_i, \quad i = 1,2,\dots,m \quad (6)$$

The weight adjustment ensures that the speed of the corresponding Krill dynamically influences the influence of each ZRP performance metric in the objective function. This dynamic weighting mechanism aligns with the KHO algorithm's adaptability, where the movement of Krill affects the emphasis on specific optimization goals.

The objective function considers the impact of the ZRP parameters updated during the Initialization step. Let $R_z$denote the zone radius, $S_i$represent the step size associated with Krill i, and $Z_i$signify the zone assignment for node i. The objective function adapts to these parameters, emphasizing the role of spatial characteristics and zone assignments in the overall optimization process:

$$Spatial\ Influence: F_i = \frac{1}{S_i}.\frac{R_z}{Z_i}, \quad i = 1,2,\dots,m \quad (7)$$

This spatial influence term ensures that the objective function accounts for the spatial distribution of nodes and the impact of zone assignments on the ZRP's performance.

3.3. Initializing Krill Population

The third step in the KHO-ZRP algorithm focuses on creating the krill population, a pivotal aspect of the KHO process. The population, denoted as P, comprises individuals representing potential solutions within the optimization framework. Each krill individual is characterized by a set of parameters, contributing to the diverse solutions for space exploration. The Initialization of the krill population involves assigning values to these parameters based on predefined criteria. Let X_i represent the position of krill i in the solution space, C_{max} denote the maximum speed of Krill, and S_{max} represent the maximum step size. Mathematically, the initialization process can be expressed as Eq.(8).

$$\begin{aligned} &Krill\ Position\ Initialization: X_i = Random(X_{min}, X_{max}), \quad i = 1,2,\dots,P \\ &Krill\ Speed\ Initilization: C_i = Random(0, C_{max}), \quad i = 1,2,\dots,P \\ &Step\ Size\ Initialization: S_i = Random(0, S_{max}), \quad i = 1,2,\dots,P \end{aligned} \quad (8)$$

Eq.(8) outlines the stochastic nature of the krill population initialization, reflecting the inherent randomness in the exploration process. The random function generates values within specified ranges, ensuring diversity in the initial population.

In the context of the ZRP, assigning nodes to zones plays a crucial role in the network's performance. During the Initialization of the krill population, each Krill is associated with a particular zone. Let Z

represent the total number of zones, Z_i signify the assigned zone for krill i, and N denote the number of nodes. The zone assignment can be mathematically expressed as Eq.(9).

$$Zone\ Assignment: Z_i = argmin_j\left(\sqrt{(X_i - X_j)^2}\right), \quad i = 1,2,\dots,P \tag{9}$$

Eq.(9) ensures that the spatial distribution of nodes is considered during the Initialization, aligning with the ZRP's reliance on local interactions within defined zones. The fitness of each Krill in the population is crucial for the subsequent stages of the optimization process. Fitness is determined by evaluating the performance of the ZRP with the parameters represented by the Krill. Let f_i denote the fitness of krill i, w_i represent the weight associated with krill i, and F_i signify the spatial influence factor. The fitness evaluation is mathematically expressed as Eq.(10).

$$Fitness\ Evaluation: f_i = w_i.F_i, \quad i = 1,2,\dots,P \tag{10}$$

Eq.(10) incorporates the weight associated with each Krill and the spatial influence factor, providing a quantitative measure of the solution's fitness. Once the fitness of each Krill is evaluated, a selection mechanism determines which Krill will proceed to the next generation. This process involves probabilistic selection based on the fitness values. Let r represent a random number between 0 and 1, and P_{select} denote the probability of selection. The krill selection equation is given by Eq.(11).

$$Krill\ Selection: Select\ Krill\ i\ if\ r < P_{select} \tag{11}$$

The probabilistic nature of Eq.(11) ensures that Krill, with higher fitness values, are more likely to be selected for the next generation. As the krill population evolves, the ZRP parameters are updated to reflect the characteristics of the chosen Krill. Let R_z denote the zone radius, S_i represent the step size associated with Krill i, and Z_i signify the zone assignment for node i. The updated equations are as Eq.(12).

$$Zone\ Radius\ Update: R_z = Average(S_i), \quad i = 1,2,\dots,P \tag{12}$$

$$Step\ Size\ Update: S_i = Average(C_i), \quad i = 1,2,\dots,P$$

$$Zone\ Assignment\ Update: Z_i = argmin_j\left(\sqrt{(X_i - X_j)^2}\right), \quad i = 1,2,\dots,P$$

Eq.(12) depicts the adjustment of ZRP parameters based on the characteristics of the selected krill population, ensuring the alignment of the ZRP with the evolving optimization process.

3.4. Evaluate Fitness

The fourth step in the KHO-ZRP algorithm involves evaluating the fitness of each Krill in the population. The fitness assessment is integral to the KHO process, as it quantifies how well each solution, represented by a krill, aligns with the optimization goals defined by the ZRP. The fitness evaluation begins with integrating the objective function, $f(ZRP)$, defined in the earlier steps. The objective function captures the essence of the ZRP's performance, considering various metrics such as energy efficiency, delay minimization, and packet delivery ratio. The fitness, f_i, of krill i is calculated as Eq.(13).

$$f_i = w_i.f(ZRP_i), \quad i = 1,2,\dots,P \tag{13}$$

where w_i represents the weight associated with krill i, adjusting the contribution of each Krill to the overall fitness based on its characteristics. The objective function $f(ZRP_i)$ encapsulates the performance of the ZRP with the parameters represented by krill i.

Considering the spatial characteristics introduced in the Initialization step, the fitness evaluation incorporates the spatial influence factor F_i. This factor emphasizes the impact of node distribution and zone assignments on the ZRP's performance. The adjusted fitness, f_i, is given by Eq.(14).

$$f_i = f_i.F_i, \quad i = 1,2,\dots,P \tag{14}$$

This adjustment ensures that the fitness of each Krill reflects not only the ZRP's overall performance but also its spatial adaptability within the network. The speed of

each Krill, denoted as C_i, is a crucial parameter in KHO-ZRP. The speed influences the exploration of the solution space and, consequently, the optimization process. The contribution of krill speed to fitness is expressed in Eq.(15).

$$f_i = f_i + \alpha . C_i, \quad i = 1,2, \ldots, P \qquad (15)$$

where α represents a scaling factor that controls the impact of krill speed on fitness, this addition acknowledges the importance of exploration and adaptability introduced by the movement of Krill within the optimization framework.

The weight w_i associated with each Krill contributes to the overall fitness evaluation. The weights are dynamically adjusted based on the speed of the Krill, ensuring that faster-moving Krill have a more pronounced impact on the overall optimization process. The weight adjustment equation is given by Eq.(16).

$$wi=wmin+Wmax-WminN.Ci, \quad i=1,2,\ldots,P \qquad (16)$$

This dynamic adjustment aligns with the KHO algorithm's adaptability, where faster-moving individuals influence collective behaviour more. The final step in the fitness evaluation process involves summing up the adjusted fitness values for all Krill in the population. The total fitness, denoted as F_{total}, is given by Eq.(17).

$$F_{total} = \sum_{i=1}^{P} f_i \qquad (17)$$

Eq.(17) provides a comprehensive measure of the krill population's overall fitness, considering the individual Krill's diverse contributions based on their parameters and spatial characteristics.

Algorithm 1. Evaluate Fitness

Input:

- P - Population size
- w_i - Weight associated with Krill i
- $f(ZRP_i)$ - Objective function value for Krill i
- F_i - Spatial influence factor for Krill i
- C_i - Speed of Krill i
- α - Scaling factor
- W_{min}- Maximum weight
- W_{max} - Maximum weight
- N - Total number of nodes

Output:

- F_{total} - Total fitness of the krill population

Procedure:

1. For each Krill i in the population P:
   a) Calculate $f_i$using the formula $f_i = w_i . f(ZRP_i)$
   b) Adjust f_i by multiplying it with F_i
   c) Add $\alpha \cdot C_i$ to f_i
   d) Dynamically adjust the weight $w_i$using the formula $w_i = W_{min} + \left(\frac{W_{max}-W_{min}}{N}\right) . C_i$
2. **Sum up the adjusted fitness values:**
   a) Calculate F_{total}as the sum of all f_i values obtained in step 1.

3.5. Update Krill Movement

The fifth step in the KHO-ZRP algorithm revolves around updating the movement of each Krill within the population. This process is crucial for KHO's adaptation and exploration capabilities and is guided by various parameters influencing the movement dynamics. Let X_i denote the current position of krill i, C_i represent its speed and S_i signify the step size. The position update equation is given by Eq.(18).

$$X_i = X_i + C_i . S_i \qquad (18)$$

Eq.(18) reflects the movement of the Krill in the solution space, where the current position, speed, and step size determine the new position. It encapsulates the exploration aspect of KHO, where Krill move through the solution space in search of optimal solutions. The speed of each Krill, C_i, is a critical factor influencing its movement. The speed update equation introduces inertia and social influence parameters. Let ω represent the inertia weight, $\emptyset_1$ denote the cognitive parameter and $\emptyset_2$ signify the social parameter. The speed update equation is expressed as Eq.(19).

$$C_i = \omega . C_i + \emptyset_1 . r_1 . (X_{best} - X_i) + \emptyset_2 . r_2 . (X_{global\_best} - X_i) \quad (19)$$

where r_1 and r_2 are random values between 0 and 1, and X_{best} and X_{global_best} represent the best position found by Krill and the best global position among all Krill.

The step size, S_i, is adjusted based on the current fitness of the Krill. Let F_i denote the fitness of krill i, and β represents the step size control parameter. The step size adaptation equation is given by Eq.(20).

$$S_i = S_i . exp\left(-\beta . \frac{F_i}{F_{total}}\right) \quad (20)$$

Eq.(20) ensures that Krill with higher fitness values contributes to smaller step sizes, emphasizing exploitation in promising regions of the solution space. A boundary check is performed after the position update to maintain the feasibility of krill positions within the solution space. A krill's position is reset to the boundary value if it exceeds predefined boundaries. The boundary check equation is expressed as Eq.(21).

$$X_i = min(max(X_i, X_{min}), X_{max}) \quad (21)$$

where X_{min} and X_{max} represent the minimum and maximum boundaries of the solution space, ensuring that krill positions are constrained within valid regions.

Limits are imposed on each Krill's speed and step size to control the exploration and exploitation trade-off. These limits prevent excessive exploration or exploitation, contributing to a balanced search process. The speed and step size limit equations are given by Eq.(22).

$$C_i = min(max(C_i, C_{min}), C_{max}) \quad S_i = min(max(S_i, S_{min}), S_{max}) \quad (22)$$

where C_{min}, C_{max} and S_{max} represent the minimum and maximum limits for speed and step size, respectively.

3.6. Environmental Influence

This step addresses the influence of external forces on Krill's movement. These forces, representing the environmental influence, contribute to shaping the trajectory of each Krill within the optimization landscape. The interaction between Krill and the environment is characterized by external forces acting on each Krill. Let $F_{external,i}$ denote the external force affecting Krill i, and M_i represent the mass of krill i. The equation describing the impact of external forces is expressed as Eq.(23).

$$F_{external,i} = M_i . A_i \quad (23)$$

where, A_i signifies the acceleration experienced by krill i due to external influences. This equation emphasizes the direct relationship between the external force and the mass of the Krill, reflecting the Newtonian principles governing the motion of objects under external forces.

Environmental gradients significantly determine the direction and intensity of external forces acting on the krill population. Let G_i represent the environmental gradient affecting Krill i, and ∇G_i denote the gradient vector. The equation describing the influence of environmental gradients is given by Eq.(24).

$$F_{external,i} = G_i . \nabla G_i \quad (24)$$

Eq.(24) incorporates both the magnitude and direction of the environmental gradient, indicating that krill experience forces directed away from regions of higher ecological gradients. The negative sign reflects the force acting in the opposite direction of the gradient. The velocity of each Krill, V_i, is influenced by its current velocity and the external forces acting on it. Let $F_{external,i}$ denote the external force on krill i, and Δt represents the time step. The velocity update equation is expressed as Eq.(25).

$$V_i = V_i + \frac{F_{external,i}}{M_i} . \Delta t \quad (25)$$

Eq.(25) reflects the change in velocity based on the external force, considering the Krill's mass. The time step, Δt is introduced to represent the discrete nature of the optimization process. The position of each Krill, X_i, is updated considering the influence of external forces on its velocity. Let V_i represent the velocity of krill i, and Δt denote the time step. The position update equation with environmental influence is given by Eq.(26)

$$X_i = X_i + V_i . \Delta t \quad (26)$$

Eq.(26) accounts for the impact of external forces on the movement of Krill, contributing to the exploration and adaptation capabilities within the optimization process. Considering the environmental influence, a boundary check is performed after the position update to ensure the feasibility of krill positions within the solution space. A krill's position is reset to the boundary value if it exceeds predefined boundaries. The boundary check equation is expressed as Eq.(27).

$$X_i = min\big((X_i, X_{min}), X_{max}\big) \quad (27)$$

Where X_{min} and X_{max} represent the minimum and maximum boundaries of the solution space, ensuring that krill positions are constrained within valid regions even with the influence of external forces.

Algorithm 2. Environmental Influence

Input:

- P - Population size
- M_i–Mass of Krill i
- A_i - Acceleration experienced by Krill i
- G_i - Environmental gradient affecting Krill i
- ∇G_i–Gradient vector for Krill i
- V_1 - Velocity of Krill i
- X_i – Position of Krill i
- Δt - Time step
- X_{min} - Minimum boundary of the solution space
- X_{max} - Maximum boundary of the solution space

Output:

- Updated position X_i for each Krill

Procedure

Step 1: Calculate the external force $F_{external,i}$

Step 2: Determine the impact of environmental gradients on the external force

Step 3: Update the velocity of Krill i considering the external force

Step 4: Update the position of krill i based on the updated velocity

Step 5: Perform a boundary check for the position X_i

3.7. Update ZRP

Step 7 of the KHO-ZRP algorithm focuses on the dynamic adaptation of ZRP parameters. The zone radius, denoted as R_z, undergoes continuous adjustments based on the characteristics of the evolving krill population. The average speed of all Krill is calculated to align the ZRP with the movement dynamics of the krill population. Let C_i represent the speed of krill i, and N denote the total number of Krill. The average speed (C_{avg}) is determined as Eq.(28).

$$C_{avg} = \frac{1}{N}\sum_{i=1}^{N} C_i \quad (28)$$

Eq.(28) captures the collective behaviour of the krill population by averaging their speeds. The ZRP adapts by incorporating this average speed in the subsequent calculations. The dynamic adjustment of the zone radius (R_z) involves scaling the average krill speed (C_{avg}) by a factor (γ). The updated zone radius is calculated using the equation Eq.(29).

$$R_z = \gamma . C_{avg} \quad (29)$$

where γ represents a scaling factor that influences the extent to which the zone radius adapts to the collective speed of the krill population. This adaptive mechanism ensures that the ZRP parameters remain synchronized with the evolving optimization process.

In the context of ZRP, the step size (S_i) associated with each Krill is crucial for the spatial organization of the network. The step size is updated based on the average krill speed (C_{avg}) and a step size control parameter (β). The step size update equation is given by Eq.(30).

$$S_i = \frac{C_{avg}}{\beta} \quad (30)$$

Eq.(30) ensures that the step size reflects the average speed of the krill population while considering the control parameter (β) to maintain a balance between exploration and exploitation. The assignment of nodes to zones is a fundamental aspect of ZRP. The updated zone radius influences the spatial organization

(R_z), step size (S_i), and the position of each Krill(X_i). The zone assignment (Z_i) for Krill, i is determined using Eq.(31).

$$Z_i = argmin_j\left(\sqrt{(X_i - X_j)^2}\right) \quad (31)$$

Eq.(31) ensures that the nodes are assigned to zones based on their proximity to the positions of the Krill in the solution space. The zone assignment's dynamic nature adapts to the krill population's changing positions. To maintain the feasibility of ZRP parameters, boundary constraints are applied to the zone radius (R_z), step size (S_i), and the average krill speed (C_{avg}). These constraints prevent unrealistic values that may arise during the optimization process. Eq.(32) gives the boundary check equations to Eq.(34).

$$R_z = min(max(R_z, R_{min}), R_{max}) \quad (32)$$

$$S_i = min(max(S_i, S_{min}), S_{max}) \quad (33)$$

$$C_{avg} = min(max(C_{avg}, C_{min}), C_{max}) \quad (34)$$

Eq.(32) to Eq.(34) ensure that the ZRP parameters maintain realistic values within specified limits, contributing to the stability of the optimization process.

3.8. Evaluate ZRP

The eighth step of the KHO-ZRP algorithm focuses on evaluating the Zone Routing Protocol (ZRP) performance.

3.8.1. Packet Delivery Ratio (PDR)

The Packet Delivery Ratio (PDR), a crucial metric reflecting packet transmission efficiency, is calculated as the ratio of successfully delivered packets to the total number of generated packets. Mathematically, PDR is defined as Eq.(35), and it provides insights into the effectiveness of the routing strategy employed by ZRP, considering both successful and unsuccessful packet deliveries.

$$PDR = \frac{Successfully\ Delivered\ Packets}{total\ Number\ of\ Packets} \quad (35)$$

3.8.2. Energy Efficiency

Energy efficiency is a critical aspect of wireless networks. The energy consumption of ZRP is assessed by considering the energy spent on successful packet delivery and the energy consumed by idle nodes. The energy consumption $(E_{consumed})$ is given by Eq.(36).

$$E_{consumed} = \sum_{i=1}^{N} E_i + \sum_{j=1}^{M} E_{idle,j} \quad (36)$$

where E_i represents the energy spent by node i on successful packet delivery and $E_{idle,j}$ represents the energy consumed by idle node j. This evaluation metric addresses the energy implications of ZRP in the context of packet routing.

3.8.3. Delay Minimization

Reducing communication delay is a key objective in network optimization. The average delay assesses ZRP's performance $\left(Delay_{avg}\right)$ incurred in successfully delivering packets. The delay is calculated as the sum of all successfully delivered packets divided by the total number of successfully delivered packets, expressed as Eq.(37).

$$Delay_{avg} = 1/Number\ of\ Successfully\ Delivered\ Packets \quad (37)$$

where $Delay_k$ represents the delay for the k-th successfully delivered packet, providing a comprehensive measure of ZRP's performance in minimizing communication delays.

3.8.4. Connectivity Analysis

The connectivity of the network is crucial for sustaining effective communication. The number of connected nodes $(N_{connected})$ is evaluated to understand the overall network connectivity. The connectivity is determined using Eq.(38), i.e., by counting the nodes that have successfully transmitted or received packets. This metric reflects the ability of ZRP to maintain network connectivity during the optimization process.

$$N_{connected} = Number\ of\ Nodes\ with\ Successful\ Packet\ Transmission \quad (38)$$

3.8.5. Routing Overhead

Routing overhead measures the additional data the routing protocol introduces

to manage the network. In ZRP, routing overhead $(O_{routing})$ is calculated as the ratio of the total number of routing control packets to the total number of successfully delivered packets. Eq.(39) quantifies the efficiency of the routing control mechanism in ZRP, indicating the extent of additional data introduced for network management.

$$O_{routing} = \frac{Total\ Number\ of\ Routing\ Control\ Packets}{Number\ of\ Successfully\ Delivered\ Packets} \quad (39)$$

3.8.6. Performance Index

To provide a comprehensive assessment, a performance index (PI) is defined as a weighted sum of the evaluated metrics. Let $w_{PDR}, w_{energy}, w_{delay}, w_{connectivity}$, and $w_{overhead}$ represent the weights assigned to the corresponding metrics. The performance index is given by Eq.(40).

$$PI = w_{PDR}.PDR + w_{energy}.E_{consumed} + w_{delay}.Delay_{avg} + w_{connectivity}.N_{connected} - w_{overhead}.O_{routing} \quad (40)$$

This composite metric captures the overall performance of ZRP by balancing the importance of various evaluated parameters.

3.9. Fitness Evaluation

Fitness Evaluation involves the critical task of evaluating the fitness of the entire system, considering the performance metrics derived in the previous steps. The objective function(f_{total}) is a comprehensive measure that integrates various performance metrics, each weighted based on its significance. Mathematically, the objective function is defined as Eq.(41).

$$f_{total} = w_{PDR}.PDR + w_{energy}.E_{consumed} + w_{delay}.Delay_{avg} + w_{connectivity}.N_{connected} - w_{overhead}.O_{routing} \quad (41)$$

where $w_{PDR}, w_{energy}, w_{delay}, w_{connectivity}$ and $w_{overhead}$ represent the weights associated with the respective performance metrics, and each term contributes to the system's overall fitness.

To enhance adaptability, the weights assigned to the performance metrics are dynamically adjusted based on the fitness of the krill population. Let W_i denote the weight associated with krill i, and F_i represent the fitness of krill i. The dynamic weight adjustment equation is given by Eq.(42).

$$W_i = W_{min} + \left(\frac{W_{max} - W_{min}}{N}\right).F_i \quad (42)$$

Eq.(42) ensures that Krill with higher fitness values significantly influence the overall fitness evaluation, promoting a dynamic and adaptive optimization process. Tracking the global best fitness (F_{global_best}) is essential for evaluating the performance of the entire system. The global best fitness is updated based on the fitness values of individual Krill, ensuring that the best-performing solution is retained. The update equation is expressed as Eq.(43).

$$F_{global_{best}} = max\left(F_{global\_best}, max_{i=1}^{N} F_i\right) \quad (43)$$

Eq.(43) captures the highest fitness value among all Krill in the population, reflecting the global best fitness achieved throughout the optimization process. Considering the dynamic nature of the optimization process, individual krill fitness values (F_i) are adjusted based on their contribution to the overall system fitness. The adjusted fitness for krill i is given by Eq.(44).

$$F_i = f_{total}.W_i \quad (44)$$

Eq.(44) incorporates the overall system fitness and the dynamically adjusted weight of the Krill, providing a nuanced evaluation of each individual's contribution to the optimization process. To ensure that fitness values remain within a reasonable range, a fitness scaling operation is applied. The scaled fitness (F_{scaled}) is calculated by normalizing the adjusted fitness values across the entire krill population:

$$F_{scaled,i} = \frac{F_i}{\sum_{j=1}^{N} F_j} \quad (45)$$

Eq.(45) guarantees that the fitness values maintain their relative proportions, facilitating a fair comparison and preventing any dominance of particular individuals in the fitness evaluation.

Algorithm 3. Fitness Evaluation

Input:

- N - Population size
- $w_{PDR}, w_{energy}, w_{delay}, w_{connectivity},$ - Weights for performance metrics
- W_{min} , W_{max} - Minimum and maximum weights for dynamic adjustment
- F_{global_best} - Global best fitness
- F_i - Fitness of Krill i for each i in the population
- f_{total} - Overall objective function value for the system

Output:

- Updated weights W_i for each Krill
- Updated global best fitness F_{global_best}
- Adjusted fitness values F_i for each Krill

Procedure:

Step 1: **Compute Objective Function:** Calculate the overall objective function value f_{total} using the weighted sum of performance metrics.

Step 2: **Dynamic Weight Adjustment:** Adjust the weights (W_i) for each Krill dynamically based on their fitness values and the specified weight range.

Step 3: **Update Global Best Fitness:** Update the global best fitness $\left(F_{global\_best}\right)$ by selecting the maximum fitness value among all Krill.

Step 4: **Krill Fitness Adjustment:** Adjust the fitness values (F_i) each Krill incorporates the overall system fitness and the dynamically adjusted weight.

Step 5: **Fitness Scaling:** Scale the adjusted fitness values to ensure they remain within a reasonable range and maintain relative proportions.

3.10. Select Krill for Next Generation

The process of selecting Krill for the next generation is crucial to drive the evolution of the population. Fitness proportional selection favours Krill with higher fitness values, increasing their likelihood of being chosen for reproduction. The probability $(P_i)$of selecting krill i is given by:

$$P_i = \frac{F_i}{\sum_{j=1}^{N} F_j} \quad (46)$$

where F_i represents the adjusted fitness value of krill i, and the sum in the denominator encompasses the total fitness of the entire population. This approach ensures that Krill with higher fitness values are more likely to be selected.

The roulette wheel selection mechanism is employed to actualize the fitness-proportional selection. A roulette wheel is constructed, with each Krill's slice proportional to its probability of selection. The spinning wheel determines the Krill chosen for the next generation. The selection process is stochastic, replicating the natural selection concept. The probability of Krill i being selected $\left(P_{select,i}\right)$ is calculated as Eq.(47).

$$P_{select,i} = \frac{P_i}{\sum_{k=1}^{N} P_k} \quad (47)$$

To control the number of offspring produced by each selected Krill, a reproduction rate $(R_i)$is introduced. This rate influences the number of offspring a krill generates, allowing for diversity in the next generation. The reproduction rate is calculated as Eq.(48).

$$R_i = \frac{F_i}{\sum_{k=1}^{N} F_j} \quad (48)$$

Eq.(48) aligns with the fitness-proportional approach, ensuring that Krill with higher fitness contribute more significantly to the next generation. The actual number of offspring produced by each Krill (O_i) is determined based on the product of its reproduction rate and a scaling factor (S). The equation for the number of offspring is given by Eq.(49).

$$O_i = \lfloor R_i \,.\, S \rfloor \quad (49)$$

where S represents the scaling factor, and the floor function ensures that the number of

offspring is an integer, reflecting the discrete nature of reproduction.

To maintain the influence of top-performing Krill in the population, a preservation mechanism is introduced. A certain percentage (P_{elite}) of the fittest Krill, based on their adjusted fitness values, is preserved directly for the next generation. The number of elite Krill preserved $(N_{elite})$is calculated as Eq.(50).

$$N_{elite} = \lfloor P_{elite} . N \rfloor \quad (50)$$

Eq.(50) ensures that a fraction of the top-performing Krill remains unchanged in the next generation. The total number of Krill in the next generation $(N_{next\_generation})$ is the sum of the preserved elite Krill and offspring from the selected Krill. Mathematically, it is expressed as Eq.(51) and captures the next generation's composition, considering both preserved elite Krill and the offspring generated by the selected Krill.

$$N_{next\_generation} = N_{elite} + \sum_{i=1}^{N} O_i \quad (51)$$

3.11. Crossover/Recombination

In Step 11 of the KHO-ZRP algorithm, the crossover or recombination process involves the selection of krill pairs for mating. This step is critical in introducing genetic diversity to the next generation. Two Krill are selected based on their adjusted fitness values and the probability of selecting Krill i as part of a mating pair $(P_{malte,i})$ is determined using the fitness-proportional selection mechanism, i.e., Eq.(52)

$$P_{mate,i} = \frac{F_i}{\sum_{j=1}^{N} F_j} \quad (52)$$

To control the likelihood of crossover occurring between selected krill pairs, a crossover rate (C_i) is introduced for each Krill. The crossover rate is calculated using Eq.(53) which is the ratio of the adjusted fitness value (F_i) to the total fitness of the entire population.

$$C_i = \frac{F_i}{\sum_{j=1}^{N} F_j} \quad (53)$$

This crossover rate influences the probability of a krill engaging in the crossover process during reproduction. The crossover point in the genetic material of the Krill is determined randomly. The crossover point $(P_{crossover})$ is selected within the range of genetic information length, allowing for the exchange of genetic material. The equation for determining the crossover point is expressed as Eq.(54).

$$P_{crossover} = random(Genetic\ Information\ Length) \quad (54)$$

The actual crossover operation involves the exchange of genetic material between the selected krill pairs. The offspring's genetic information is created by combining the genetic material of the parent krill up to the crossover point. The genetic material exchange equation is given by Eq.(55).

$$Offspring\ Genetic\ Information = \{Parent\ 1\ Genetic\ Information = Combine\ Genetic\ Material\ of\ Patent\ 1\ and\ Patent\ 2\ up\ to\ P_{cr} \quad (55)$$

Eq.(55) introduces variations in the offspring's genetic information, contributing to genetic diversity in the population. The sum of offspring from all mating pairs determines the number of offspring produced by the crossover operation. The offspring population size $(N_{offspring})$ is calculated as Eq.(56). and it represents the sum of offspring produced by each krill pair during the crossover process.

$$N_{offspring} = \sum_{i=1}^{N} O_i \quad (56)$$

The composition of the next generation is established by combining the offspring from the crossover process with the preserved elite Krill from the previous generation. The total number of Krill in the next generation $(N_{next\_generation})$ is given by Eq.(57).

$$N_{next_{generation}} = N_{elite} + N_{offspring} \quad (57)$$

Eq.(57) captures the total population size in the next generation, ensuring that both preserved elite Krill and offspring contribute to the genetic diversity and evolution of the population.

3.12. Mutation

In Step 12 of the KHO-ZRP algorithm, the mutation process introduces stochastic changes to the genetic material of Krill in the population. The probability of a krill undergoing mutation $(P_{mutation,i})$ is determined based on Krill's adjusted fitness value. The mutation probability is calculated using the fitness-proportional selection mechanism. Eq.(58) reflects the likelihood of mutation for each Krill in the population.

$$P_{mutation,i} = \frac{F_i}{\sum_{j=1}^{N} F_j} \quad (58)$$

To control the overall mutation rate in the population, a mutation rate (M_i) is introduced for each Krill. The mutation rate is calculated as the ratio of the adjusted fitness value (F_i) To the entire population's total fitness, expressed as Eq.(59), it influences the probability of a krill undergoing mutation during the optimization process.

$$M_i = \frac{F_i}{\sum_{j=1}^{N} F_j} \quad (59)$$

The mutation point within the genetic material of a krill is determined randomly. The mutation point $(P_{mutation})$ is selected within the range of genetic information length, allowing for the introduction of random variations. The equation for determining the mutation point is Eq.(60).

$$P_{mutation} = random(Genetic\ Information\ Length) \quad (60)$$

The actual mutation operation involves introducing random variations to the genetic material of a krill at the selected mutation point. The mutation process is modelled as Eq.(61), and it introduces randomness to the genetic material, promoting diversity in the population.

$$Mutated\ Genetic\ Information = Random\ Variation\ Introduced\ at\ P_{mutation} \quad (61)$$

Creating mutated offspring for Krill selected for mutation involves applying the mutation operation to their genetic material. The mutated offspring's genetic information is produced by introducing random variations at the mutation point. The equation for generating mutated offspring is expressed as Eq.(62).

$$Mutated\ Offspring\ Genetic\ Information = Mutated\ Genetic\ Information\ of\ Parent \quad (62)$$

Eq.(62) ensures that the offspring inherits the mutated genetic material from its parent, contributing to the evolution of the population. The composition of the next generation is established by combining the mutated offspring with the preserved elite Krill from the previous generation. The total number of Krill in the next generation $(N_{next_generation})$is given by Eq.(63).

$$N_{next_{generation}} = N_{elite} + N_{mutated\_offspring} \quad (63)$$

where $N_{mutated\_offspring}$ represents the total number of Krill produced through the mutation process. This equation captures the next generation's full population size, integrating preserved elite Krill and mutated offspring.

3.13. Survival Selection

In Step 13 of the KHO-ZRP algorithm, survival selection involves determining the probability of each Krill surviving to the next generation. The survival probability $(P_{survival,i})$ is calculated based on the adjusted fitness values of the Krill. The survival probability is expressed as Eq.(64) using the fitness-proportional selection mechanism.

$$P_{survival,i} = \frac{F_i}{\sum_{j=1}^{N} F_j} \quad (64)$$

Eq.(64) reflects the likelihood of each Krill surviving based on its performance during optimization. To control the overall survival rate in the population, a survival rate (S_i) is introduced for each Krill. The survival rate is calculated as the ratio of the adjusted fitness value (F_i) to the total fitness of the entire population.

$$S_i = \frac{F_i}{\sum_{j=1}^{N} F_j} \quad (65)$$

Eq.(65) influences the probability of each Krill surviving the selection process for the next generation. The survival selection

process involves comparing the survival probability of each Krill with a random threshold value. If the survival probability exceeds the threshold, the Krill is selected to survive; otherwise, it is eliminated. The survival selection equation is given by Eq.(66).

$$Survival\ Status_i = \{1,\ if\ P_{survival,i} > random(0,1)\ 0,\ otherwise \quad (66)$$

where $Survival\ Status_i$ indicates whether krill i survives (1) or not (0) based on the comparison with the random threshold.

To ensure the preservation of the top-performing Krill, a fraction (P_{elite}) of the fittest individuals is directly preserved for the next generation. The number of elite Krill preserved (N_{elite}) is calculated as Eq.(67).

$$N_{elite} = \lfloor P_{elite}.N \rfloor \quad (67)$$

Eq.(67) ensures that a fraction of the top-performing Krill remains unchanged in the next generation. The survival status of each Krill determines the composition of the next generation. To adaptively control the krill density in the population, a control parameter $(D_{adaptive})$ is introduced. The adaptive krill density control equation is expressed as Eq.(68).

$$D_{adaptive} = \frac{N_{next\_generation}}{N} \quad (68)$$

This parameter reflects the proportion of the population that survives to the next generation, influencing the overall population density.

3.14. Termination Criteria

Termination criteria in Step 14 of the KHO-ZRP algorithm aim to decide when the optimization process should conclude. A common criterion is convergence, assessing whether the algorithm has reached a stable state. The convergence criteria equation is defined as Eq.(69).

$$Convergence\ Criteria = \text{Previous Best} - \text{Current Best} \quad (69)$$

where $Best\ Objective\ Function\ Value_{current}$ and $Best\ Objective\ Function\ Value_{previous}$ represent the best objective function values in the current and previous iterations. The convergence criteria evaluate the relative change in the best objective function value.

Another termination criterion is based on a predefined maximum number of iterations (I_{max}). The optimization process terminates when the current iteration surpasses this predefined maximum. The maximum iterations criteria are expressed as Eq.(70).

$$Maximum\ Iteration\ Criteria = \{1,\ if\ I_{current} \geq I_{max}\ 0,\ otherwise \quad (70)$$

where, $I_{current}$ represents the current iteration, and the termination criteria return 1 if the maximum iterations are reached.

Stagnation criteria assess whether the optimization process has stagnated, indicating that further iterations might not lead to substantial improvements. It involves monitoring the change in the best objective function value over a specified number of iterations.

rations $(I_{stagnation})$. The stagnation criteria equation is given by Eq.(71).

$$Stagnation\ Criteria = (abs(Best\ Objective\ Function\ Value_{current} - Best\ Objective\ Function\ Value_{previous})/ Best\ Objective\ Function\ Value_{previous} \quad (71)$$

where the stagnation threshold is a predefined value, and the termination criteria are satisfied if the change in the best objective function value is below this threshold for the specified number of iterations.

Terminating based on achieving a target objective value (Target Objective) is another criterion. Optimization concludes when the best objective function value reaches or surpasses this predefined target. The aim of target value criteria is given by Eq.(72).

$$Target\ Objective\ Criteria = \{1,\ if\ Best\ Objective\ Function\ Value_{current} \geq Target\ Objective\ 0,\ otherwise \quad (72)$$

This criterion checks whether the optimization process has met or exceeded the

target objective. The final termination decision involves a combination of the individual termination criteria. A logical OR operation is applied to determine whether any requirements have been met, indicating that the optimization process should terminate. The termination decision equation is expressed as Eq.(73).

$$Termination\ Decision = Convergence\ Criteria\ OR\ Maximum\ Iterations\ Criteria\ OR\ Stagnation\ Criteria \quad (73)$$

where the termination decision is 1 if any of the individual termination criteria are satisfied, and 0 otherwise.

Algorithm 4. KHO-ZRP

Input:

- Objective Function
- ZRP Parameters
- Termination Criteria
- Population Size (N)
- Krill Movement Parameters
- Crossover and Mutation Parameters
- Environmental Parameters

Output:

- Optimal ZRP Parameters
- Performance Metrics
- Converged Krill Population

Procedure:

Step 1: **Initialization**
- Initialize Krill Population Positions, Velocities, and ZRP Parameters.

Step 2: **Define Objective Function**
- Formulate the Objective Function considering ZRP Performance Metrics.

Step 3: **Initialize Krill Population**
- Generate an initial population of Krill with random positions and velocities.

Step 4: **Evaluate Fitness**
- Evaluate the fitness of each Krill based on the defined objective function.

Step 5: **Update Krill Movement**
- Update the positions and velocities of Krill using the Krill Movement equations.

Step 6: **Environmental Influence**
- Apply environmental influence to adjust Krill's movement towards better solutions.

Step 7: **Update ZRP Parameters**
- Adjust ZRP Parameters based on the performance of the krill population.

Step 8: **Evaluate ZRP Performance**
- Evaluate the performance of the ZRP using the updated parameters.

Step 9: **Fitness Evaluation**
- Reevaluate the fitness of Krill considering the updated ZRP Performance.

Step 10: **Select Krill for Next Generation**
- Use fitness-proportional and roulette wheel selection to choose Krill for reproduction.
- Determine the number of offspring each Krill produces.

Step 11: **Crossover/Recombination**
- Select pairs of Krill for mating based on their adjusted fitness.
- Introduce crossover to exchange genetic material and create offspring.

Step 12: **Mutation:**
- Apply mutation to introduce random variations in the genetic material of Krill.

Step 13: **Survival Selection:**
- Determine the survival of Krill based on their adjusted fitness.
- Preserve a fraction of elite Krill for the next generation.

Step 14: Termination Criteria:

- Check convergence, maximum iterations, stagnation, and target objective criteria.
- Exit the optimization process if any termination criterion is met; otherwise, repeat Step 5.

This algorithm outlines the iterative optimization process of KHO-ZRP, combining krill movement, environmental influence, and genetic operators like crossover and mutation. The termination criteria ensure that the algorithm stops when a satisfactory solution is achieved, or certain conditions are met.

3.15. Experimental Reproducibility and Methodological Clarity

The experimental methodology follows a structured and repeatable workflow enabling independent replication. Network topology initialization defines UAV count, spatial boundaries, mobility model, transmission range, and initial energy values as listed in Table 2. Zone Routing Protocol parameters include initial zone radius, hello interval, routing mode selection, and neighbor discovery configuration. Krill Herd Optimization parameters include population size, step size bounds, velocity limits, inertia weight, crossover rate, mutation rate, elite preservation ratio, and termination thresholds. These parameters remain fixed across comparative evaluations.

Simulation execution follows a deterministic sequence. Krill population initialization precedes objective function computation using delay, packet delivery ratio, packet loss ratio, throughput, and energy consumption metrics. Iterative optimization updates krill movement, environmental influence, crossover, mutation, and survival selection until termination criteria satisfaction. Updated krill solutions directly map to ZRP parameter adaptation at each iteration. Performance metrics are collected using identical traffic models, node densities, simulation duration, and random seed control across all protocols.

This methodological specification ensures experiment repeatability through consistent parameter disclosure, deterministic execution order, and uniform evaluation conditions, supporting independent validation and comparative benchmarking.

4. SIMULATION SETTING

NS3, a discrete-event network simulator, is a pivotal tool in FANET research, offering a versatile and robust platform for exploring the complexities of aerial communication systems. Its modular architecture and extensive library of models enable researchers to simulate diverse scenarios, encompassing varying node mobility patterns, communication protocols, and network topologies. Researchers unravel insights into FANET behavior through meticulous parameter configuration, scrutinizing factors like node positioning algorithms, routing protocols, and network performance metrics. Moreover, NS3's open-source nature fosters collaboration and innovation, nurturing a vibrant ecosystem of knowledge exchange within the research community. Its expansive documentation and active user base provide ample support for researchers at all levels, facilitating experimentation and discovery in FANETs. In essence, NS3 stands as an indispensable ally, transcending the constraints of physical experimentation to offer a virtual playground where researchers can delve into the intricacies of aerial communication systems, paving the way for advancements in this burgeoning field. The settings used for conducting the simulation in this research are provided in Table 2.

Table 2: Simulation Settings

Parameter	Value
Antenna Model	Omnidirectional
Carrier Frequency	2.4 GHz
Communication Standard	IEEE 802.11n
Data Rate	2 Mbps
Data Size	1024 bits
Flight Speed of Nodes	10-40 m/s
Initial Energy	1000 J
Mobility Model	3D GM
Network Density	20-100 nodes
Network Scenario Size	5000 m * 5000 m * 700 m
Packet Sending Rate	5 packets/s

Path Energy Consumption Factor (η)	0.1 pJ/(bit*m^2)
Propagation Radius	1200 m
Simulation Software	NS3
Traffic Model	Constant Bit Rate (CBR)
Transmission Energy Consumption Factor (EEM)	4 nJ/bit
Transmission Power (Pt)	15 dBm
Transmission Radius	250 m
Transport Protocol	UDP
Update Interval of the Hello Message (ΔT)	3 s

5. RESULTS AND DISCUSSIONS

5.1. Delay Evaluation

Delay in Flying Ad Hoc Networks (FANETs) refers to the time data packets travel from the source to the destination. It encompasses various factors such as transmission, propagation, queuing, and processing delays. Minimizing delay is crucial in FANETs to ensure timely and reliable communication between unmanned aerial vehicles (UAVs). In Figure 1, the x-axis represents the number of UAVs in the network, while the y-axis illustrates the delay in milliseconds (ms). This visualization depicts how the delay changes with varying network sizes, offering insights into protocol performance and scalability.

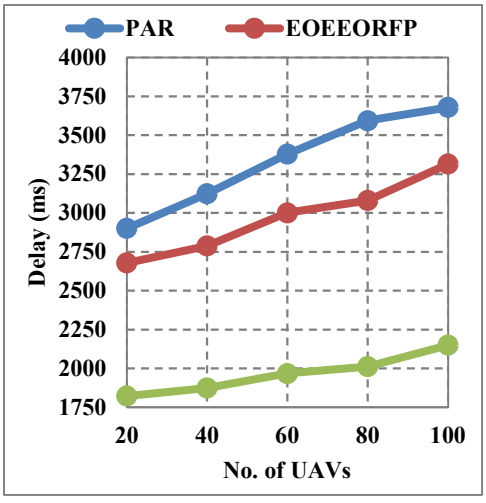

Figure 1. Delay Trend Analysis

PAR, with an average delay of 3334.6 ms, exhibits a steady increase in delay as the number of UAVs rises. This trend highlights the protocol's challenge in adapting to larger network sizes, leading to increased processing and decision-making times. PAR leverages deep reinforcement learning to predict network conditions and adaptively adjust routing decisions. However, the computational complexity of predicting optimal routes in more extensive networks contributes to the observed delay increase. Despite its delay challenges, PAR's adaptive routing approach holds promise for optimizing FANET communication by dynamically responding to changing network conditions.

EOEEORFP maintains a relatively stable delay trend with an average delay of 2971.8 ms across different UAV counts. This consistency reflects the protocol's efficiency in balancing energy consumption and route quality, ensuring consistent performance in varying network sizes. EOEEORFP prioritizes energy efficiency and security in route selection, resulting in stable delay values. The protocol's ability to maintain consistent performance contributes to its reliability in FANET environments, where energy conservation and secure data transmission are paramount.

KHO-ZRP demonstrates superior performance with an average delay of 1964.4 ms. Despite an increase in network size, KHO-ZRP exhibits a notable decrease in delay, showcasing its adaptability and efficiency in dynamically adjusting routes based on environmental conditions and network density. KHO-ZRP incorporates Krill Herd Optimization to enhance routing efficiency, enabling it to minimize delay effectively. By dynamically adjusting routes based on real-time network conditions, KHO-ZRP optimizes data transmission paths, reducing delay and improving overall network performance. The protocol's superior performance underscores the effectiveness of incorporating advanced optimization techniques like Krill Herd Optimization in FANET routing protocols.

Table 3. Delay Summary

No. of UAVs	PAR	EOEEORFP	KHO-ZRP
20	2901	2678	1822
40	3122	2787	1873
60	3378	3000	1967
80	3593	3079	2011
100	3679	3315	2149
Average	**3334.6**	**2971.8**	**1964.4**

The delay trends of PAR, EOEEORFP, and KHO-ZRP, as illustrated by their average delay values, provide valuable insights into protocol performance in varying FANET scenarios. KHO-ZRP emerges as the most efficient protocol, highlighting the significance of incorporating advanced optimization techniques like Krill Herd Optimization in FANET routing protocols to minimize delay and enhance network performance. These findings underscore the importance of protocol-specific optimizations in addressing the unique challenges of aerial communication networks.

5.2. Packet Delivery Ratio Assessment

Packet Delivery Ratio (PDR) in Flying Ad Hoc Networks (FANETs) refers to the ratio of successfully delivered packets to the total number of packets sent within the network. It measures the reliability and efficiency of data transmission, indicating the percentage of packets that reach their intended destinations without loss or error. In Figure 2, the x-axis represents the number of UAVs in the network, while the y-axis illustrates the Packet Delivery Ratio (PDR) as a percentage (%). This visualization provides insights into how the PDR changes with varying network sizes, offering a measure of protocol performance and reliability.

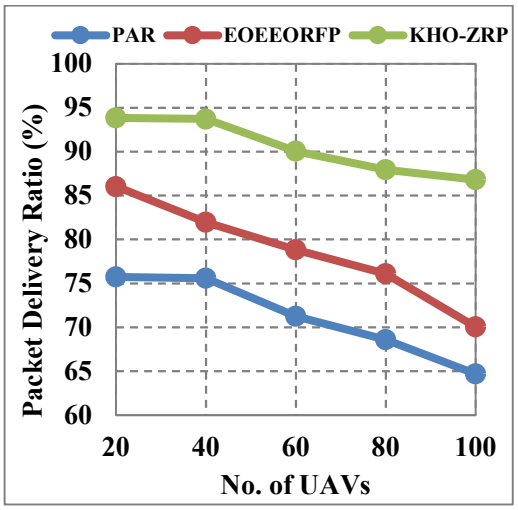

Figure 2. Packet Delivery Ratio Trends

PAR exhibits a decreasing trend in PDR as the number of UAVs increases. This decline can be attributed to the limitations of its prediction-supported adaptive routing mechanism in accurately anticipating optimal routes in more extensive and dynamic networks. The protocol's reliance on predictions may lead to suboptimal route selections, decreasing reliability and packet delivery rates. Despite its sophisticated deep reinforcement learning approach, PAR's predictive models may struggle to adapt to the complexities of real-time network dynamics, impacting its PDR performance negatively. EOEEORFP, while emphasizing energy efficiency and secure route selection, may work to efficiently respond to sudden changes in network topology or environmental factors. The protocol's optimization for optimal route finding prioritizes energy efficiency over real-time adaptability, potentially leading to reduced reliability in data transmission. Consequently, EOEEORFP maintains relatively stable PDR values but may face challenges maintaining high delivery rates in dynamic FANET environments. Its focus on energy optimization and security may compromise its ability to dynamically adjust routes, impacting its overall PDR performance, especially in scenarios with rapidly changing network conditions.

KHO-ZRP demonstrates superior performance in PDR across varying network sizes. Its integration of Krill Herd Optimization enables it to dynamically adjust routes based on real-time environmental conditions and

network density. By leveraging the collective intelligence of the krill herd optimization algorithm, KHO-ZRP optimizes data transmission paths, resulting in higher packet delivery rates and improved overall network reliability. This adaptability and efficiency in route selection contribute to KHO-ZRP's advantages in achieving consistently high PDR values, making it a robust choice for data transmission in FANETs. Its ability to adapt to changing network conditions and optimize routes based on real-time data distinguishes it from PAR and EOEEORFP, enabling it to maintain high PDR values even in challenging FANET environments.

Table 4. Packet Delivery Summary

No. of UAVs	PAR	EOEEORFP	KHO-ZRP
20	75.731	86.023	93.850
40	75.575	81.953	93.702
60	71.245	78.812	90.034
80	68.586	76.080	87.931
100	64.702	70.060	86.809
Average	**71.167**	**78.585**	**90.465**

Figure 2 highlights the Packet Delivery Ratio trends of PAR, EOEEORFP, and KHO-ZRP in varying FANET scenarios. While PAR and EOEEORFP may face challenges adapting to dynamic network conditions, KHO-ZRP stands out with its superior performance in achieving high packet delivery rates. The protocol's integration of Krill Herd Optimization enhances its adaptability and efficiency in route selection, contributing to its advantages in ensuring reliable data transmission in FANET environments. These findings underscore the importance of advanced optimization techniques in optimizing FANET routing protocols and improving network reliability and performance.

5.3. Packet Loss Ratio Assessment

Packet Loss Ratio (PLR) in FANETs is a critical metric representing the percentage of packets lost during transmission compared to the total sent. It's a key indicator of network reliability and performance, crucial for assessing the effectiveness of routing protocols in ensuring data delivery. Figure 3 depicts how PLR changes with varying numbers of UAVs in the network. The x-axis signifies the number of UAVs, while the y-axis denotes PLR as a percentage. This visualization allows us to discern trends in packet loss as the network scales, providing insights into protocol performance under different conditions.

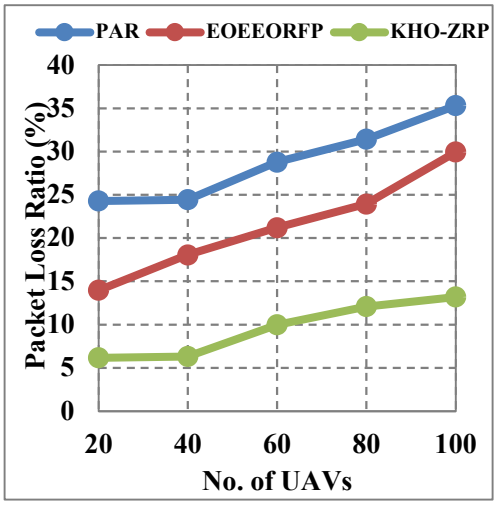

Figure 3. Packet Loss Ratio Analysis

PAR exhibits a concerning trend of increasing PLR with the expansion of the network. At 20 UAVs, PAR records a PLR of 24.270%, which escalates to 35.299% at 100 UAVs. This rise in PLR suggests that PAR may encounter difficulties adapting its routing decisions effectively as the network grows. While innovative, the protocol's reliance on prediction-supported adaptive routing may introduce inaccuracies or delays in route selection, leading to a higher incidence of packet loss. Additionally, PAR's deep reinforcement learning mechanism may struggle to accurately predict optimal routes in dynamic and complex FANET environments, further contributing to increased packet loss rates. EOEEORFP demonstrates relatively consistent PLR values across different network sizes. Although minor fluctuations occur, the protocol maintains PLR levels lower than PAR. For example, at 20 UAVs, EOEEORFP's PLR is 13.978%, increasing slightly to 29.941% at 100 UAVs. This suggests that EOEEORFP delivers a more stable performance in mitigating packet loss. However, its

optimization for energy-efficient routing may prioritize specific routes over others, potentially resulting in increased packet loss in specific network scenarios. Despite this, EOEEORFP's focus on energy efficiency and secure data transmission contributes to its effectiveness in minimizing packet loss in FANET environments.

KHO-ZRP is the most promising protocol for minimizing packet loss across all network sizes. With consistently lower PLR values compared to PAR and EOEEORFP, KHO-ZRP demonstrates robustness in ensuring reliable data transmission. For instance, at 20 UAVs, KHO-ZRP's PLR stands at 6.150%, rising modestly to 13.192% at 100 UAVs. This superior performance can be attributed to its integration of Krill Herd Optimization, which facilitates dynamic route adjustments based on real-time environmental conditions and network density. By leveraging advanced optimization techniques, KHO-ZRP optimizes data transmission paths to minimize packet loss, even in challenging FANET environments with high node mobility or network congestion.

Table 5. Packet Loss Summary

No. of UAVs	PAR	EOEEORFP	KHO-ZRP
20	24.270	13.978	6.150
40	24.426	18.048	6.298
60	28.756	21.189	9.967
80	31.415	23.921	12.07
100	35.299	29.941	13.192
Average	**28.833**	**21.415**	**9.535**

The analysis underscores the pivotal role of protocol-specific optimizations in addressing packet loss in FANETs. While PAR may grapple with scalability and adaptive routing decisions, EOEEORFP maintains stability but may lack adaptability in specific scenarios. Conversely, KHO-ZRP's integration of advanced optimization techniques enables it to consistently minimize packet loss, highlighting the potential of innovative routing protocols to enhance FANET reliability and performance. As FANETs evolve, further research and development efforts are warranted to refine existing protocols and develop novel solutions that address the unique challenges of packet loss mitigation in dynamic aerial communication networks.

5.4. Throughput Evaluation

Throughput in FANETs refers to the rate at which data packets are successfully transmitted from source to destination within the network. It measures the network's capacity to deliver data effectively and is typically expressed in data packets per unit of time. The graph illustrates the relationship between the number of UAVs in the network and the corresponding throughput performance. The x-axis represents the quantity of UAVs deployed in the network, while the y-axis indicates throughput measured in data packets per unit time. Analyzing this graph provides insights into how throughput varies as the network scales, enabling the assessment of protocol performance and network capacity.

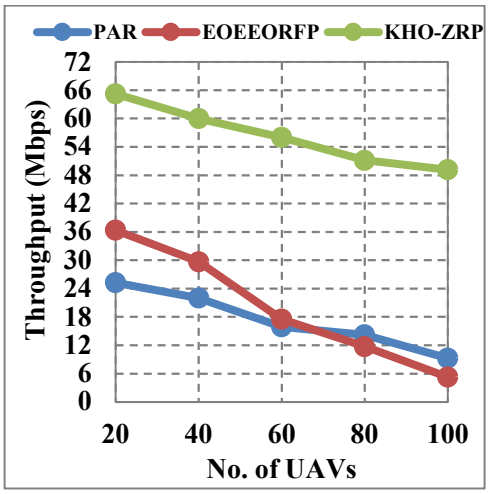

Figure 4. Throughput Performance

PAR exhibits a decreasing trend in throughput as the network size expands. At 20 UAVs, PAR achieves a throughput of 25.244 packets, which decreases to 9.279 packets at 100 UAVs. This decline may be attributed to PAR's prediction-supported adaptive routing mechanism, which faces challenges adapting to more extensive networks. As the number of UAVs increases, PAR may struggle to accurately predict optimal routing paths, resulting in suboptimal decisions and reduced data transmission rates. Consequently, the protocol may experience higher congestion and packet loss levels, further impacting throughput. Despite its innovative approach to adaptive routing, PAR's reliance on predictive models may hinder its performance in dynamically changing FANET environments,

particularly in high network density and mobility scenarios.

EOEEORFP demonstrates relatively stable throughput performance across different network sizes. At 20 UAVs, EOEEORFP achieves a throughput of 36.323 packets, decreasing slightly to 5.227 packets at 100 UAVs. This consistency in throughput suggests that EOEEORFP maintains stable data transmission rates, contributing to its reliability in delivering packets. However, its optimization for energy-efficient routing may prioritize certain routes over others, potentially impacting throughput in specific network scenarios. Despite this, EOEEORFP's focus on energy efficiency and secure data transmission enhances its effectiveness in minimizing packet loss and ensuring reliable data delivery in FANETs.

KHO-ZRP emerges as the top performer in throughput across all network sizes. With consistently higher throughput values compared to PAR and EOEEORFP, KHO-ZRP demonstrates robustness in data transmission. For instance, at 20 UAVs, KHO-ZRP achieves a throughput of 65.221 packets, which declines slightly to 49.145 at 100 UAVs. This superior performance can be attributed to its integration of Krill Herd Optimization, which optimizes route selection based on real-time environmental conditions and network density, enhancing data transmission rates and throughput. By dynamically adjusting routing decisions, KHO-ZRP mitigates congestion and packet loss, ensuring efficient and reliable data delivery in FANETs.

Table 6. Throughput Summary

No. of UAVs	PAR	EOEEORFP	KHO-ZRP
20	25.244	36.323	65.221
40	21.965	29.659	59.987
60	15.892	17.493	55.998
80	14.186	11.713	51.138
100	9.279	5.227	49.145
Average	**17.313**	**20.083**	**56.298**

The analysis highlights the significance of protocol-specific optimizations in achieving high throughput in FANETs. While PAR may face challenges in scalability and adaptive routing decisions, EOEEORFP's energy-efficient approach may limit its throughput potential. In contrast, KHO-ZRP's integration of advanced optimization techniques enables it to consistently achieve higher throughput, showcasing its potential to enhance FANET reliability and performance. As FANETs continue to evolve, further research and development efforts are essential to refine existing protocols and develop innovative solutions that maximize throughput while addressing the unique challenges of aerial communication networks.

5.5. Energy Consumption Assessment

Energy consumption in FANETs refers to the amount of power UAVs consume during operation. It is a critical factor in determining the endurance and overall performance of UAVs in FANETs, as higher energy consumption rates can lead to shorter flight durations and reduced mission capabilities. The graph depicts the relationship between the number of UAVs in the network and their corresponding energy consumption levels. The x-axis represents the quantity of UAVs deployed in the network, while the y-axis indicates energy consumption measured in percentage such as watt-hours or battery capacity percentage. Analyzing this graph provides insights into how energy consumption varies as the network scales, enabling the assessment of protocol efficiency and its impact on UAV endurance.

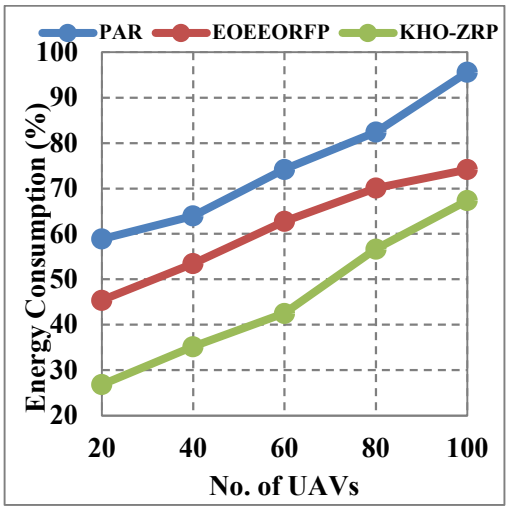

Figure 5. Energy Consumption Trends

PAR exhibits a steady increase in energy consumption as the network size expands. At 20 UAVs, PAR consumes 58.887%

of energy, which rises to 95.551% at 100 UAVs. This trend may be attributed to PAR's prediction-supported adaptive routing mechanism, which requires continuous monitoring and analysis of network conditions to make informed routing decisions. PAR may expend more energy on predictive modeling and decision-making processes as the network grows, resulting in higher energy consumption rates. Additionally, the protocol's reliance on deep reinforcement learning algorithms may contribute to increased computational overhead, further elevating energy consumption levels.

EOEEORFP demonstrates relatively lower energy consumption compared to PAR across different network sizes. At 20 UAVs, EOEEORFP consumes 45.380% of energy, increasing to 74.156% at 100 UAVs. This indicates that EOEEORFP's optimization for energy-efficient routing enables it to conserve power more effectively than PAR. EOEEORFP reduces the energy expended by UAVs during communication tasks by prioritizing energy-efficient routes and minimizing unnecessary data transmissions. Consequently, the protocol enhances UAV endurance and prolongs mission durations, making it suitable for applications requiring prolonged aerial operations.

KHO-ZRP demonstrates the lowest energy consumption levels among the three protocols across all network sizes. With energy consumption values significantly lower than PAR and EOEEORFP, KHO-ZRP exhibits superior energy efficiency in FANETs. At 20 UAVs, KHO-ZRP consumes 26.837% of energy, increasing to 67.293% at 100 UAVs. This remarkable efficiency can be attributed to integrating Krill Herd Optimization, which optimizes route selection based on real-time environmental conditions and network density. By selecting energy-efficient routes and minimizing unnecessary energy expenditure, KHO-ZRP maximizes UAV endurance and extends mission capabilities, making it an ideal choice for energy-constrained FANET applications.

Table 6. Energy Consumption Summary

No. of UAVs	PAR	EOEEORFP	KHO-ZRP
20	58.887	45.380	26.837
40	63.938	53.420	35.148
60	74.171	62.719	42.461
80	82.378	70.056	56.645
100	95.551	74.156	67.293
Average	**74.985**	**61.146**	**45.677**

The analysis underscores the importance of protocol-specific optimizations in minimizing energy consumption and enhancing UAV endurance in FANETs. While PAR may experience higher energy consumption rates due to its complex decision-making processes, EOEEORFP's optimization for energy-efficient routing enables it to conserve power effectively. However, KHO-ZRP is the most energy-efficient protocol, leveraging advanced optimization techniques to minimize energy expenditure and maximize UAV endurance. As FANETs evolve, further research and development efforts are essential to refine existing protocols and develop innovative solutions that optimize energy consumption while ensuring reliable communication and mission success.

5.6. Limitations, Literature Perspectives, and Result Analysis Justification

The proposed KHO-ZRP framework presents measurable improvements across delay, packet delivery, packet loss, throughput, and energy metrics under simulated ultra-dynamic FANET conditions. Still, certain limitations remain. The evaluation relies on simulation-based environments using predefined mobility and traffic models. Real-world aerial disturbances, hardware-level constraints, and environmental uncertainties are not directly captured. The optimization process introduces additional computational overhead, which may affect real-time responsiveness under extremely dense UAV deployments. Scalability beyond the evaluated node range also requires further empirical validation.

Existing literature presents differing viewpoints on FANET routing design. Learning-driven protocols emphasize adaptive intelligence but often incur higher computational and energy costs. Purely bio-inspired approaches favor lightweight decision mechanisms but may lack predictive capability under abrupt topology variation. Geographic and clustering-based protocols report stability benefits but struggle under rapid three-dimensional mobility. These contrasting perspectives highlight the absence of a unified

routing strategy that balances adaptability, stability, and energy efficiency under extreme mobility.

The result analysis criteria adopted in this study align with widely accepted FANET evaluation practices. Delay, packet delivery ratio, packet loss ratio, throughput, and energy consumption directly reflect mission-critical communication requirements in UAV swarms. Comparative evaluation against PAR and EOEEORFP follows consistent simulation settings, node densities, and traffic patterns to ensure fairness. Metric selection prioritizes routing-layer behavior, stability under density variation, and energy sustainability, matching the intended scope of routing-centric contribution.

Reported FANET studies focus either on learning-driven adaptability with higher delay and energy cost or bio-inspired routing with limited stability under rapid density variation. The presented results demonstrate that KHO-ZRP attains lower delay, higher packet delivery, reduced packet loss, improved throughput, and controlled energy usage across increasing node density under uniform simulation settings. The research contribution differs by embedding krill herd optimization directly into zone radius control, relay selection, and hop regulation inside a single routing architecture. Achievement of research objectives is validated through sustained routing stability and energy efficiency trends that address performance gaps highlighted in existing literature, confirming advancement at the routing-system design level rather than isolated metric improvement.

6. CONCLUSION

The integration of Krill Herd Optimization (KHO) into the Zone Routing Protocol (ZRP) has shown significant promise in addressing the complex routing challenges of Flying Ad Hoc Networks (FANETs). The KHO-ZRP protocol offers a dynamic and adaptive solution for efficiently navigating UAVs through dynamic airspace with varying node densities and environmental conditions. By leveraging KHO's optimization techniques, KHO-ZRP enhances real-time routing decisions, minimizing delays, packet loss, and energy consumption. Simulation-based evaluations demonstrate its superiority over existing protocols, consistently delivering improved performance across various network sizes. The results underscore KHO-ZRP's potential to enhance routing efficiency and reliability in FANETs, providing a promising solution for ensuring reliable communication in dynamic and challenging aerial environments. Further research could explore enhancements such as refining KHO parameters or integrating machine learning algorithms to enhance adaptability and resilience, thus solidifying KHO-ZRP's position as a leading solution for reliable communication in dynamic and challenging aerial environments.

REFERENCES

[1] N. Mansoor, M. I. Hossain, A. Rozario, M. Zareei, and A. R. Arreola, “A Fresh Look at Routing Protocols in Unmanned Aerial Vehicular Networks: A Survey,” *IEEE Access*, vol. 11, pp. 66289–66308, 2023, doi: 10.1109/ACCESS.2023.3290871.

[2] J. Sharma and P. S. Mehra, “Secure communication in IOT-based UAV networks: A systematic survey,” *Internet of Things (Netherlands)*, vol. 23, p. 100883, 2023, doi: 10.1016/j.iot.2023.100883.

[3] J. Zhang *et al.*, “Aeronautical Ad Hoc Networking for the Internet-Above-The-Clouds,” *Proc. IEEE*, vol. 107, no. 5, pp. 868–911, 2019, doi: 10.1109/JPROC.2019.2909694.

[4] M. Gharib, F. Afghah, and E. S. Bentley, “LB-OPAR: Load balanced optimized predictive and adaptive routing for cooperative UAV networks,” *Ad Hoc Networks*, vol. 132, p. 102878, 2022, doi: 10.1016/j.adhoc.2022.102878.

[5] M. U. Farooq and M. Zeeshan, “Connected dominating set enabled on-demand routing (CDS-OR) for wireless mesh networks,” *IEEE Wirel. Commun. Lett.*, vol. 10, no. 11, pp. 2393–2397, 2021, doi: 10.1109/LWC.2021.3101476.

[6] X. Wei, H. Yang, and W. Huang, “Low-Delay Routing Scheme for UAV Communications in Smart Cities,” *IEEE Internet Things J.*, vol. 10, no. 21, pp. 18837–18843, 2023, doi: 10.1109/JIOT.2023.3267131.

[7] M. Zhang, C. Dong, P. Yang, T. Tao, Q. Wu, and T. Q. S. Quek, “Adaptive Routing Design for Flying Ad Hoc

Networks," *IEEE Commun. Lett.*, vol. 26, no. 6, pp. 1438–1442, 2022, doi: 10.1109/LCOMM.2022.3152832.

[8] F. H. Kumbhar and S. Y. Shin, "Innovating Multi-Objective Optimal Message Routing for Unified High Mobility Networks," *IEEE Trans. Veh. Technol.*, vol. 72, no. 5, pp. 6571–6583, 2023, doi: 10.1109/TVT.2022.3232567.

[9] M. A. Al-Absi, A. A. Al-Absi, M. Sain, and H. Lee, "Moving ad hoc networks—a comparative study," *Sustain.*, vol. 13, no. 11, 2021, doi: 10.3390/su13116187.

[10] C. Han, J. Yin, L. Ye, and Y. Yang, "NCAnt: A Network Coding-Based Multipath Data Transmission Scheme for Multi-UAV Formation Flying Networks," *IEEE Commun. Lett.*, vol. 25, no. 3, pp. 1041–1044, 2021, doi: 10.1109/LCOMM.2020.3039846.

[11] T. Bilen and B. Canberk, "Q-Learning Driven Routing for Aeronautical Ad-Hoc Networks," *Pervasive Mob. Comput.*, vol. 87, p. 101724, 2022, doi: 10.1016/j.pmcj.2022.101724.

[12] Saifullah, Z. Ren, K. Hussain, and M. Faheem, "K-means online-learning routing protocol (K-MORP) for unmanned aerial vehicles (UAV) adhoc networks," *Ad Hoc Networks*, vol. 154, p. 103354, 2024, doi: 10.1016/j.adhoc.2023.103354.

[13] S. M. Bozorgi, M. Golsorkhtabaramiri, S. Yazdani, and S. Adabi, "A smart optimizer approach for clustering protocol in UAV-assisted IoT wireless networks," *Internet of Things (Netherlands)*, vol. 21, p. 100683, 2023, doi: 10.1016/j.iot.2023.100683.

[14] L. Guezouli, K. Barka, and A. Djehiche, "UAVs's efficient controlled mobility management for mobile heterogeneous wireless sensor networks," *J. King Saud Univ. - Comput. Inf. Sci.*, vol. 34, no. 6, pp. 2461–2470, 2022, doi: 10.1016/j.jksuci.2020.09.017.

[15] S. Swain, P. M. Khilar, and B. R. Senapati, "A reinforcement learning-based cluster routing scheme with dynamic path planning for mutli-UAV network," *Veh. Commun.*, vol. 41, p. 100605, 2023, doi: 10.1016/j.vehcom.2023.100605.

[16] Y. Cui, Q. Zhang, Z. Feng, Z. Wei, C. Shi, and H. Yang, "Topology-Aware Resilient Routing Protocol for FANETs: An Adaptive Q-Learning Approach," *IEEE Internet Things J.*, vol. 9, no. 19, pp. 18632–18649, 2022, doi: 10.1109/JIOT.2022.3162849.

[17] O. T. Abdulhae, J. S. Mandeep, and M. Islam, "Cluster-Based Routing Protocols for Flying Ad Hoc Networks (FANETs)," *IEEE Access*, vol. 10, pp. 32981–33004, 2022, doi: 10.1109/ACCESS.2022.3161446.

[18] Y. Cui, H. Tian, C. Chen, W. Ni, H. Wu, and G. Nie, "New Geographical Routing Protocol for Three-Dimensional Flying Ad-Hoc Network Based on New Effective Transmission Range," *IEEE Trans. Veh. Technol.*, vol. 72, no. 12, pp. 16135–16147, 2023, doi: 10.1109/TVT.2023.3296082.

[19] A. Chowdhury and D. De, "RGSO-UAV: Reverse Glowworm Swarm Optimization inspired UAV path-planning in a 3D dynamic environment," *Ad Hoc Networks*, vol. 140, p. 103068, 2023, doi: 10.1016/j.adhoc.2022.103068.

[20] D. Mallikarachchi, K. S. Wong, and J. M. Y. Lim, "Covert communication in multi-hop UAV network," *Ad Hoc Networks*, vol. 128, p. 102788, 2022, doi: 10.1016/j.adhoc.2022.102788.

[21]. J. Ramkumar and R. Vadivel, "Improved frog leap inspired protocol (IFLIP) – for routing in cognitive radio ad hoc networks (CRAHN)," World J. Eng., vol. 15, no. 2, pp. 306–311, 2018, doi: 10.1108/WJE-08-2017-0260.

[22]. J. Ramkumar and R. Vadivel, "Improved Wolf prey inspired protocol for routing in cognitive radio Ad Hoc networks," Int. J. Comput. Networks Appl., vol. 7, no. 5, pp. 126–136, 2020, doi: 10.22247/ijcna/2020/202977.

[23]. K. S. J. Marseline, J. Ramkumar, and D. R. Medhunhashini, "Sophisticated Kalman Filtering-Based Neural Network for Analyzing Sentiments in Online Courses," in Smart Innovation, Systems and Technologies, A. K. Somani, A. Mundra, R. K. Gupta, S. Bhattacharya, and A. P. Mazumdar, Eds., Springer Science and Business Media Deutschland GmbH, 2024, pp. 345–358. doi: 10.1007/978-981-97-3690-4_26.

[24]. L. Mani, S. Arumugam, and R. Jaganathan, "Performance Enhancement

of Wireless Sensor Network Using Feisty Particle Swarm Optimization Protocol," in ACM International Conference Proceeding Series, Association for Computing Machinery, 2022. doi: 10.1145/3590837.3590907.

[25]. J. Ramkumar and R. Vadivel, "CSIP—cuckoo search inspired protocol for routing in cognitive radio ad hoc networks," in Advances in Intelligent Systems and Computing, D. P. Mohapatra and H. S. Behera, Eds., Springer Verlag, 2017, pp. 145–153. doi: 10.1007/978-981-10-3874-7_14.

[26]. N. K. Ojha, A. Pandita, and J. Ramkumar, "Cyber security challenges and dark side of AI: Review and current status," in Demystifying the Dark Side of AI in Business, IGI Global, 2024, pp. 117–137. doi: 10.4018/979-8-3693-0724-3.ch007.

[27]. R. Jaganathan, S. Mehta, and R. Krishan, Intelligent Decision Making Through Bio-Inspired Optimization. IGI Global, 2024. doi: 10.4018/979-8-3693-2073-0.

[28]. J. Ramkumar, K. S. Jeen Marseline, and D. R. Medhunhashini, "Relentless Firefly Optimization-Based Routing Protocol (RFORP) for Securing Fintech Data in IoT-Based Ad-Hoc Networks," Int. J. Comput. Networks Appl., vol. 10, no. 4, pp. 668–687, 2023, doi: 10.22247/ijcna/2023/223319.

[29]. M. P. Swapna and J. Ramkumar, "Multiple Memory Image Instances Stratagem to Detect Fileless Malware," in Communications in Computer and Information Science, S. Rajagopal, K. Popat, D. Meva, and S. Bajeja, Eds., Springer Science and Business Media Deutschland GmbH, 2024, pp. 131–140. doi: 10.1007/978-3-031-59100-6_11.

[30]. M. Lingaraj, T. N. Sugumar, C. S. Felix, and J. Ramkumar, "Query aware routing protocol for mobility enabled wireless sensor network," Int. J. Comput. Networks Appl., vol. 8, no. 3, pp. 258–267, 2021, doi: 10.22247/ijcna/2021/209192.

[31]. S. P. Geetha, N. M. S. Sundari, J. Ramkumar, and R. Karthikeyan, "Energy Efficient Routing In Quantum Flying Ad Hoc Network (Q-FANET) Using Mamdani Fuzzy Inference Enhanced Dijkstra's Algorithm (MFI-EDA)," J. Theor. Appl. Inf. Technol., vol. 102, no. 9, pp. 3708–3724, 2024.

[32]. R. Jaganathan, S. Mehta, and R. Krishan, Bio-Inspired intelligence for smart decision-making. IGI Global, 2024.

[33]. R. Jaganathan and V. Ramasamy, "Performance modeling of bio-inspired routing protocols in Cognitive Radio Ad Hoc Network to reduce end-to-end delay," Int. J. Intell. Eng. Syst., vol. 12, no. 1, pp. 221–231, 2019.

[34]. J. Ramkumar, R. Vadivel, and B. Narasimhan, "Constrained Cuckoo Search Optimization Based Protocol for Routing in Cloud Network," Int. J. Comput. Networks Appl., vol. 8, no. 6, pp. 795–803, 2021.

[35]. J. Ramkumar, R. Karthikeyan, and M. Lingaraj, "Optimizing IoT-Based Quantum Wireless Sensor Networks Using NM-TEEN Fusion of Energy Efficiency and Systematic Governance," in Lecture Notes in Electrical Engineering, V. Shrivastava, J. C. Bansal, and B. K. Panigrahi, Eds., Springer Science and Business Media Deutschland GmbH, 2025, pp. 141–153.

[36]. B. Suchitra, R. Karthikeyan, J. Ramkumar, and V. Valarmathi, "Enhancing Recurrent Neural Network Performance for Latent Autoimmune Diabetes Detection (Lada) Using Exocoetidae Optimization," J. Theor. Appl. Inf. Technol., vol. 103, no. 5, pp. 1645–1667, 2025.

[37]. J. Ramkumar and D. Ravindran, "Machine learning and robotics in urban traffic flow optimization with graph neural networks and reinforcement learning," in Machine Learning and Robotics in Urban Planning and Management, 2025, pp. 83–104.

[38]. R. Jaganathan, K. Rajendran, and P. S. Ponnukumar, "Peregrine Falcon Optimization Routing Protocol (PFORP) for Achieving Ultra-Low Latency and Boosted Efficiency in 6G Drone Ad-Hoc Networks (DANET)," Int. J. Comput. Digit. Syst., vol. 17, no. 1, pp. 1–18, 2025.

[39]. S. P. Priyadharshini, F. Nirmala Irudayam, and J. Ramkumar, "An Unique Overture of Plithogenic Cubic Overset, Underset and Offset," in Studies in Fuzziness and Soft Computing, vol. 435, 2025, pp. 139–156.

[40]. J. Ramkumar, B. Varun, V. Valarmathi, D. R. Medhunhashini, and R. Karthikeyan, "Jaguar-Based Routing Protocol (JRP) For Improved Reliability And Reduced Packet Loss In Drone Ad-Hoc Networks (DANET)," J. Theor. Appl. Inf. Technol., vol. 103, no. 2, pp. 696–713, 2025.

[41]. P. S. Ponnukumar, N. I. Francis Xavier, and R. Jaganathan, "Stable Plithogenic Cubic Sets," J. Fuzzy Ext. Appl., vol. 6, no. 2, pp. 410–423, 2025.

[42]. J. Ramkumar and V. Valarmathi, "Harnessing AI-Driven Models for Sustainable Development in Business Management," in World Sustainability Series, vol. Part F775, 2025, pp. 217–238.

[43]. S. P. Priyadharshini and J. Ramkumar, "Mappings Of Plithogenic Cubic Sets," Neutrosophic Sets Syst., vol. 79, pp. 669–685, 2025.

[44]. A. Senthilkumar, J. Ramkumar, M. Lingaraj, D. Jayaraj, and B. Sureshkumar, "Minimizing Energy Consumption in Vehicular Sensor Networks Using Relentless Particle Swarm Optimization Routing," Int. J. Comput. Networks Appl., vol. 10, no. 2, pp. 217–230, 2023.

[45]. J. Ramkumar, R. Karthikeyan, and K. O. Nitish, "Securing Library Data With Blockchain Advantage," in Enhancing Security and Regulations in Libraries with Blockchain Technology, 2024, pp. 117–138.

[46]. V. Valarmathi and J. Ramkumar, "Modernizing Wildfire Management Through Deep Learning and IoT in Fire Ecology," in Machine Learning and Internet of Things in Fire Ecology, 2024, pp. 203–229.

[47]. B. Suchitra, J. Ramkumar, and R. Karthikeyan, "Frog Leap Inspired Optimization-Based Extreme Learning Machine For Accurate Classification Of Latent Autoimmune Diabetes In Adults (LADA)," J. Theor. Appl. Inf. Technol., vol. 103, no. 2, pp. 472–494, 2025.

[48]. J. Ramkumar, V. Valarmathi, and R. Karthikeyan, "Optimizing Quality of Service and Energy Efficiency in Hazardous Drone Ad-Hoc Networks (DANET) Using Kingfisher Routing Protocol (KRP)," Int. J. Eng. Trends Technol., vol. 73, no. 1, pp. 410–430, 2025.

[49]. R. Jaganathan, S. Rajagopal, and K. Rajendran, "Cultural Intelligence in the AI Era-Enhancing Transitional Higher Education," in Bridging Global Divides for Transnational Higher Education in the AI Era, 2024, pp. 273–292.

[50]. J. Ramkumar, A. Senthilkumar, M. Lingaraj, R. Karthikeyan, and L. Santhi, "Optimal Approach for Minimizing Delays in Iot-Based Quantum Wireless Sensor Networks Using Nm-Leach Routing Protocol," J. Theor. Appl. Inf. Technol., vol. 102, no. 3, pp. 1099–1111, 2024.

[51]. D. Jayaraj, J. Ramkumar, M. Lingaraj, and B. Sureshkumar, "AFSORP: Adaptive Fish Swarm Optimization-Based Routing Protocol for Mobility Enabled Wireless Sensor Network," Int. J. Comput. Networks Appl., vol. 10, no. 1, pp. 119–129, Jan. 2023.

[52]. J. Ramkumar, S. S. Dinakaran, M. Lingaraj, S. Boopalan, and B. Narasimhan, "IoT-Based Kalman Filtering and Particle Swarm Optimization for Detecting Skin Lesion," in Lecture Notes in Electrical Engineering, K. Murari, N. Prasad Padhy, and S. Kamalasadan, Eds., Singapore: Springer Nature Singapore, 2023, pp. 17–27.

[53]. J. Ramkumar, C. Kumuthini, B. Narasimhan, and S. Boopalan, "Energy Consumption Minimization in Cognitive Radio Mobile Ad-Hoc Networks using Enriched Ad-hoc On-demand Distance Vector Protocol," in 2022 International Conference on Advanced Computing Technologies and Applications, ICACTA 2022, Institute of Electrical and Electronics Engineers Inc., 2022.

[54]. P. Menakadevi and J. Ramkumar, "Robust Optimization Based Extreme Learning Machine for Sentiment Analysis in Big Data," in 2022 International Conference on Advanced Computing Technologies and Applications, ICACTA 2022, Institute of Electrical and Electronics Engineers Inc., 2022.

[55]. M. P. Swapna, J. Ramkumar, and R. Karthikeyan, "Energy-Aware Reliable Routing with Blockchain Security for Heterogeneous Wireless Sensor Networks," in Lecture Notes in Networks and Systems, V. Goar, M. Kuri, R.

Kumar, and T. Senjyu, Eds., Springer Science and Business Media Deutschland GmbH, 2025, pp. 713–723.

[56]. J. Ramkumar and R. Vadivel, "Multi-Adaptive Routing Protocol for Internet of Things based Ad-hoc Networks," Wirel. Pers. Commun., vol. 120, no. 2, pp. 887–909, 2021.

[57]. R. Jaganathan and R. Vadivel, "Intelligent Fish Swarm Inspired Protocol (IFSIP) for Dynamic Ideal Routing in Cognitive Radio Ad-Hoc Networks," Int. J. Comput. Digit. Syst., vol. 10, no. 1, pp. 1063–1074, 2021.

[58]. R. Vadivel and J. Ramkumar, "QoS-enabled improved cuckoo search-inspired protocol (ICSIP) for IoT-based healthcare applications," Inc. Internet Things Healthc. Appl. Wearable Devices, pp. 109–121, 2019.

[59]. J. Ramkumar, R. Karthikeyan, and V. Valarmathi, "Alpine Swift Routing Protocol (ASRP) for Strategic Adaptive Connectivity Enhancement and Boosted Quality of Service in Drone Ad Hoc Network (DANET)," Int. J. Comput. Networks Appl., vol. 11, no. 5, pp. 726–748, 2024.

[60]. J. Ramkumar and R. Vadivel, "Whale optimization routing protocol for minimizing energy consumption in cognitive radio wireless sensor network," Int. J. Comput. Networks Appl., vol. 8, no. 4, pp. 455–464, 2021.

[61]. M. P. Swapna, D. Rajeev, J. Ramkumar, and S. Chandran, "Unveiling Cybercrime Patterns in Kerala: A Machine Learning Approach," in Lecture Notes in Networks and Systems, 2026, pp. 111–122.

[62]. R. Jaganathan, S. Mehta, and R. Krishan, "Preface," Bio-Inspired Intell. Smart Decis., pp. xix–xx, 2024.

[63]. R. Jaganathan, S. Mehta, and R. Krishan, "Preface," Intell. Decis. Mak. Through Bio-Inspired Optim., pp. xiii–xvi, 2024.